Astron. Astrophys. 352, 239–247 (1999)

ASTRONOMY AND ASTROPHYSICS

The dwarf nova RZ Leonis: photometric period, "anti-humps" and normal alpha disc⋆

R.E. Mennickent[1,⋆⋆], **C. Sterken**[2], **W. Gieren**[1], **and E. Unda**[1]

[1] Universidad de Concepción, Departamento de Física, Casilla 4009, Concepción, Chile
[2] University of Brussels (VUB), Pleinlaan 2, 1050 Brussels, Belgium

Received 26 August 1999 / Accepted 15 October 1999

Abstract. We present results of differential photometry of the dwarf nova RZ Leonis spanning a 11-year baseline. The most striking feature of the light curve is a non-coherent periodic hump of variable amplitude. A seasonal time series analysis yields a photometric period of $0^{\rm d}.0756(12)$. In addition, low amplitude fluctuations of the mean magnitude in time scale of months are observed. We find that the hump's amplitude is anti-correlated with the star's mean magnitude and becomes "negative" (i.e. an absorption feature or "anti-hump") when the system is very faint. Secondary humps and "anti-humps" are also observed. The transition from "anti-humps" to fully developed humps occurs on a time scale of 70 days. We interprete the observations as a rapid response of the accretion disk to the increase of mass transfer rate. In this case we deduce a viscosity parameter $\alpha \sim 0.08$, i.e. much larger than often claimed for WZ Sge-like stars. We note that the secondary star in RZ Leo is close to a main-sequence red dwarf and not a brown-dwarf like star as suggested for other long cycle-length SU UMa stars like WZ Sge and V592 Her. Our results indicate that large amplitude and long cycle length dwarf novae might not necessarily correspond to objects in the same evolutive stage.

Key words: stars: individual: RZ Leo – stars: novae, cataclysmic variables – stars: fundamental parameters – stars: evolution – stars: binaries: general

1. Introduction: about RZ Leonis

Dwarf novae are interacting binary stars in which a Roche-lobe filling main-sequence secondary looses mass through the L_1 point. The transferred mass falls along a ballistic trajectory towards the heavier white dwarf primary, forming an accretion disk. The disk undergoes semi-periodic collapse during which matter is accreted by the compact primary. The result is a release of gravitational energy which is observed as a system brightening. This is called a dwarf nova outburst. Dwarf novae, a subclass of cataclysmic variable stars (CVs), have been reviewed by Warner (1995a).

RZ Leonis is a long cycle-length large-amplitude dwarf nova with only 7 outbursts recorded since 1918 (e.g Vanmuster & Howell 1996) and with an estimated distance from earth between 174 and 246 pc (Sproats et al. 1996).

Humps in the light curve of RZ Leo repeating with a $0^{\rm d}.0708(3)$ period were observed by Howell & Szkody (1988). They concluded that this dwarf nova is a candidate for SU UMa star probably seen under a large inclination. This assumption is supported by the finding of broad double emission-lines in the optical spectrum (Cristiani et al. 1985, Szkody & Howell 1991). Orbital humps are observed in some high-inclination dwarf novae (e.g. Szkody 1992), they probably reflect the pass of the disk-stream interacting region (often named hot spot or bright spot) along the observer's line of sight.

The study of the hot spot variability of RZ Leo is potentially useful to constrain models of gas dynamics in close binary systems. In the classical view, the hot spot is formed during the shock interaction of matter in the gaseous stream flowing from L_1 (the inner Lagrangian point) with the outer boundary of the accretion disk. This picture was consistent with photometric observations of dwarf novae during many years. However, this view conflicts with recents observations indicating anomalous hot spots in many systems. For example, in many cases, Doppler tomography does not show the effect of a hot spot at all, or indicates that the hot spot is not in the place where we would expect a collision between the gaseous stream and the outer boundary of the disk (e.g. Wolf et al. 1998). To explain these findings, the possibility of gas stream overflow has been worked out. In this view the hot spot is formed behind the white dwarf by the ballistic impact of a deflected stream passing over the white dwarf (e.g. Armitage & Livio 1998, Hessmann 1999). However, this scenario has not yet been confirmed by observations. Furthermore, recent three-dimensional numerical simulations indicate the *absence* of a shock between the stream and the disk. The interaction between the stream and the *common envelope* of the system forms and extended shock wave along the edge of the stream, whose observational properties are roughly equivalent to those of a hot spot in the disk (Bisikalo et al. 1998).

Send offprint requests to: R.E. Mennickent (rmennick@stars.cfm.udec.cl)

⋆ Based on observations obtained at Las Campanas Observatory and ESO La Silla Observatory (ESO Proposal 54.E-0812)

⋆⋆ On leave in Harvard-Smithsonian Center for Astrophysics, 60 Garden St, MA 02138, Cambridge, USA

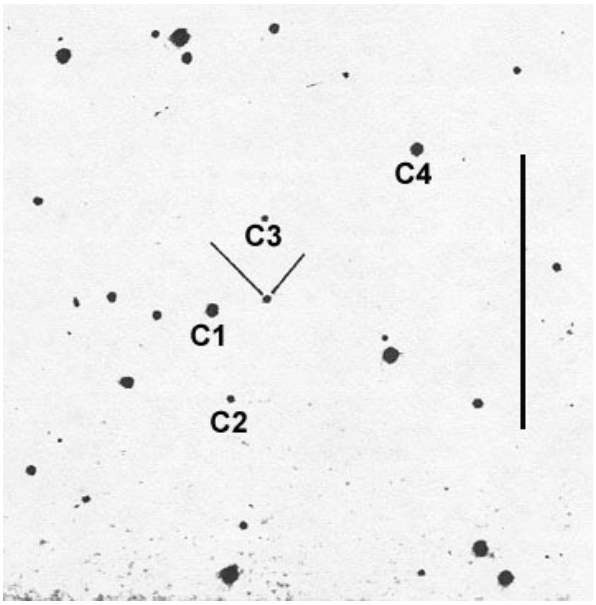

Fig. 1. The finding chart for RZ Leo. North is up and East left. Comparison and check stars are labeled. The vertical bar shows a 5-arcminute distance. Adapted from Vogt & Bateson (1982).

This paper is aimed to confirm the reported photometric period and to establish a long-term hump ephemeris. We also expect to detect systematic luminosity trends and get insights about the hump variability and hot spot nature. Interestingly, we find some phenomena conflicting, in many ways, with the classical scenario of the hot spot forming region.

2. The observations and data reduction

CCD images were obtained at six observing runs during 1991–1999 at Las Campanas Observatory (LCO) and ESO La Silla Observatory, Chile. Exposure times were between 250 and 300 s. Details of the observations are given in Table 1.

All science images were corrected for bias and were flat-fielded using standard IRAF[1] routines. Instrumental magnitudes were calculated with the *phot* aperture photometry package, which is adequate due to the RZ Leo's uncrowded field. The optimum aperture radius defined by Howell (1992) was used. This radius matches the $HWHM$ of the point spread function, minimizing the noise contribution due to sky pixels and readout noise.

In this paper we are interested in differential photometry. This technique, reviewed by Howell (1992), involves the determination of time series $V-C$ and $C-CH$, among instrumental magnitudes of variable (V), comparison (C) and check (CH) stars in the same CCD field. A finding chart of RZ Leo showing the check and comparison stars is shown in Fig. 1.

[1] IRAF is distributed by the National Optical Astronomy Observatories, which are operated by the Association of Universities for Research in Astronomy, Inc., under cooperative agreement with the National Science Foundation

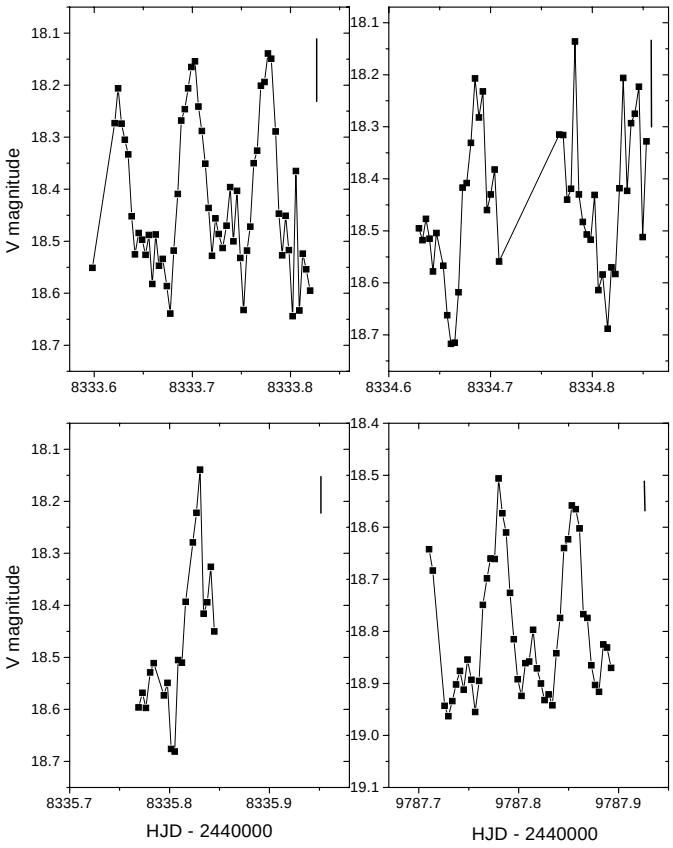

Fig. 2. Differential magnitudes on March 1991 and 1995. Note the high amplitude humps. A typical error is shown by the bar in the upper right corner of every panel.

The photometric error of $V-C$ was derived from the standard deviation of the $C-CH$ differences. In general, the intrinsic variance (not due to variability but to noise) associated to each differential light curve σ_{V-C} and σ_{C-CH} are related by a scale factor Γ depending on the relative brightness of the sources (Howell et al. 1988, Eq. 13). This factor is of order of unity if the three sources are of similar brightness or if the variable is of similar brightness to the check star and the comparison is brighter. These criteria are completely fulfilled in our observations.

Table 1 shows mean V magnitudes along with the comparison and check stars used every night. The star labeled $C1$ in Fig. 1 (for which V = 14.201 is given by Misselt 1996), was used to shift the differences to an non-differential magnitude scale. On the other hand, UBV magnitudes taken at HJD 244 8333.5981, 244 8333.6044 and 244 8333.6131 were properly calibrated with photometric standard stars, yielding V = $18\overset{\mathrm{m}}{.}56 \pm 0\overset{\mathrm{m}}{.}04$, $B-V$ = $0\overset{\mathrm{m}}{.}17 \pm 0\overset{\mathrm{m}}{.}07$ and $U-B$ = $-1\overset{\mathrm{m}}{.}02 \pm 0\overset{\mathrm{m}}{.}08$.

3. Results

3.1. The humps: a distinctive character of the light curve

The differential light curves shown in Fig. 2 indicate the presence of prominent humps on March 1991 and 1995. The humps are roughly symmetrical lasting by about 65 minutes and fol-

Table 1. Journal of observations. N is the number of science frames per night. HJD is the heliocentric julian day at the start of every sequence, referred to the zero point 244 0000. Comparison (C) and check (CH) stars are labeled accordingly to Fig. 1. The variances of the $C-CH$ differences and $V-C$ light curve and the mean magnitude of RZ Leo are also given. Note the decrease of variability associated to the faint state of Jan-Feb 1998. Setup A refers to the 1.0 m LCO telescope and B to the Dutch 0.92 m ESO telescope.

Date (UT)	HJD	N	setup	C	CH	σ_{C-CH}	σ_{V-C}	$\overline{V}$
18/03/91	8333.5981	58	A	C1	C3	$0\overset{\mathrm{m}}{.}06$	$0\overset{\mathrm{m}}{.}14$	18.42
19/03/91	8334.6296	44	A	C1	C3	$0\overset{\mathrm{m}}{.}08$	$0\overset{\mathrm{m}}{.}14$	18.45
20/03/91	8335.7690	19	A	C2	C3	$0\overset{\mathrm{m}}{.}04$	$0\overset{\mathrm{m}}{.}15$	18.47
11/03/95	9787.7102	46	A	C4	C3	$0\overset{\mathrm{m}}{.}03$	$0\overset{\mathrm{m}}{.}13$	18.80
07/01/98	10820.7488	25	B	C1	C2	$0\overset{\mathrm{m}}{.}02$	$0\overset{\mathrm{m}}{.}04$	19.08
11/01/98	10824.7719	27	B	C1	C2	$0\overset{\mathrm{m}}{.}02$	$0\overset{\mathrm{m}}{.}05$	19.13
06/02/98	10850.7540	30	B	C1	C2	$0\overset{\mathrm{m}}{.}01$	$0\overset{\mathrm{m}}{.}03$	19.06
07/02/98	10851.7520	30	B	C1	C2	$0\overset{\mathrm{m}}{.}02$	$0\overset{\mathrm{m}}{.}04$	18.94
18/03/98	10890.6939	36	B	C1	C2	$0\overset{\mathrm{m}}{.}02$	$0\overset{\mathrm{m}}{.}09$	18.71
19/03/98	10891.6219	22	B	C1	C2	$0\overset{\mathrm{m}}{.}02$	$0\overset{\mathrm{m}}{.}08$	18.67
22/01/99	11200.7394	26	B	C2	C3	$0\overset{\mathrm{m}}{.}02$	$0\overset{\mathrm{m}}{.}07$	18.71
23/01/99	11201.7722	25	B	C2	C3	$0\overset{\mathrm{m}}{.}02$	$0\overset{\mathrm{m}}{.}08$	18.63

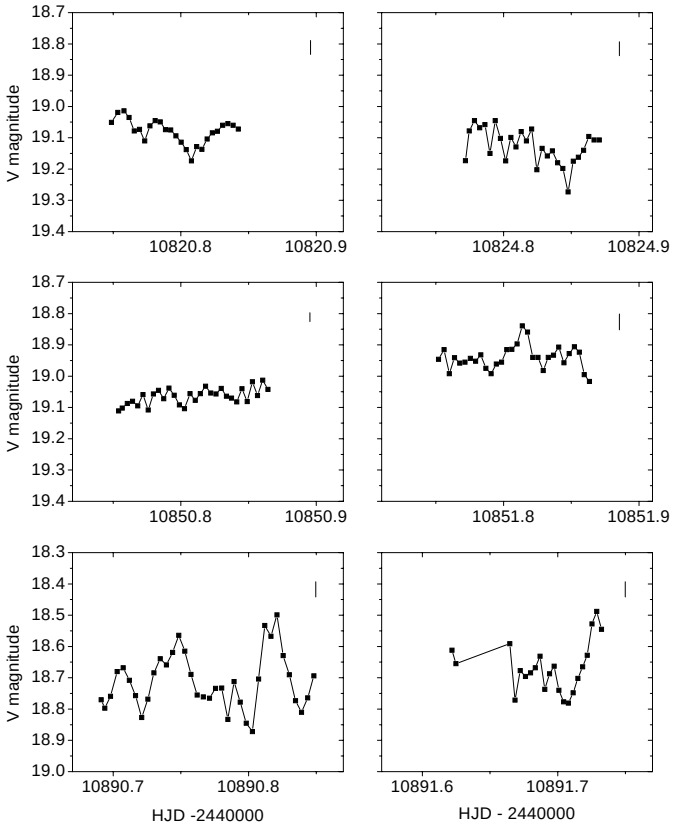

Fig. 3. Differential magnitudes at early 1998. Note the absence of humps in the upper panels and the different vertical scale in the panels. A typical error is shown by the bar in the upper right corner of every panel.

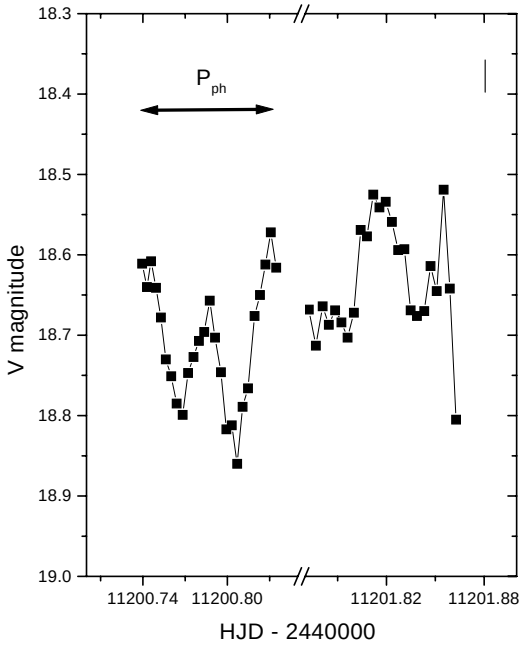

Fig. 4. Differential magnitudes on January 1999. The humps appear again. A typical error is shown by the bar in the upper right corner. The double arrow shows the length of the photometric period.

lowed by a slow magnitude decrease (March 1991) or by a secondary low-amplitude hump (March 1995). This picture sharply contrasts with that observed on early 1998 (Fig. 3). The humps are completely absent on January-February 1998 and re-appear (with secondary humps) on March 1998 and January 1999 (Fig. 4). A remarkable feature is the absorption like feature seen on January 1998. We will show in the next section that this feature is the "embrion" of the fully developed humps seen two months later.

3.2. The long-term light curve

Fig. 5 shows the long-term light curve of RZ Leo during 1987–1999. It is evident that the quiescence mean magnitude changes by several tenths of magnitude in a few years and at 3.5×10^{-3} mag d^{-1} during January and March 1998. Unfortunately, the faintness of the object has prevented a continuous monitoring, so the long-term data are inevitably undersampled.

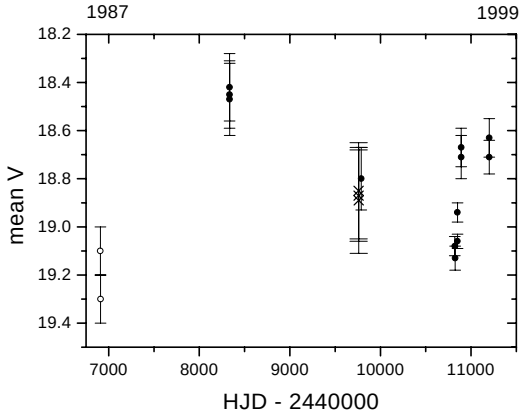

Fig. 5. Mean magnitudes of RZ Leo during 1987–1999. Error bars indicate nightly rms. Data are from Howell & Szkody (1988, open circles), Mennickent (in preparation, crosses) and this paper (solid circles).

3.3. Searching for a photometric period

We removed the long-term fluctuations normalizing the magnitudes to a common nightly mean. Then we applied the Scargle (1982) algorithm, implemented in the $MIDAS\,TSA$ package, which obeys an exponential probability distribution and is especially useful for smooth oscillations. In this statistics, the false alarm probability p_0 depends on the periodogram's power level z_0 through $z_0 \approx \ln N/p_0$, for small p_0, where N is the number of frequencies searched for the maximum power (Scargle 1982, Eq. 19). In our search we used N = 20000, so the 99% confidence level (i.e. those corresponding to p_0 = 0.01) corresponds to a power z_0 = 14.5. The range of frequency scanned was between the Nyquist frequency, i.e. 1.7 $\times 10^{-3}$ c/d and 1 c/d. After applying the method to the whole dataset many significant aliases appeared around a period $0\overset{\mathrm{d}}{.}076$. Apparently, the light curve was characterized by a non-coherent or non-periodic oscillation. We decided to start with our more restricted dataset of March 1991. The corresponding periodogram, shown in Fig. 6, shows a strong period at $0\overset{\mathrm{d}}{.}0756(12)$ (108.9 $\pm$ 1.7 m, the error correspond to the half width at half maximum of the periodogram's peak) flanked by the $\pm$ 1 c d^{-1} aliases at $0\overset{\mathrm{d}}{.}070$ (the period found by Howell & Szkody 1988) and $0\overset{\mathrm{d}}{.}082$. The ephemeris for the time of hump maximum is:

$$T_{max} = 2448333.6186(35) + 0\overset{\mathrm{d}}{.}0756(12)E \qquad (1)$$

In order to search for possible period changes we constructed a $O-C$ diagram based on timings obtained measuring the hump maxima. These timings, given in Table 2, were compared with a test period of $0\overset{\mathrm{d}}{.}0756$. The $O-C$ differences versus the cycle number are shown in Fig. 7. Apparently, the period is not changing in a smooth and predictable way. In principle, the $O-C$ differences are compatible with non-coherent humps and/or period jumps. To explore both possibilities, we searched for seasonal periods. Only datasets of March 1991, 1995 and 1998 were dense enough to construct periodograms. The results, given in Table 3, suggest a non-coherent signal rather than a variable period. In summary, the data are compatible with humps repeating with a period of $0\overset{\mathrm{d}}{.}0756(12)$ but in a non-coherent way. Armed with a photometric period, we constructed seasonal mean light curves. Only nights with fully developed humps were included. The results, shown in Fig. 8, clearly show secondary humps around photometric phase 0.5. These mean light curves are provided as a hint for future light curve modeling.

Table 2. Times of hump's maximum. HJD' means HJD - 244 0000. Measures are from our light curves shown in Figs. 2 to 4 except those indicated by † (derived from the Howell & Szkody's 1988 light curve) and †† (Mennickent, in preparation).

HJD'(maximum)	HJD'(maximum)
6909.7374(3)†	9787.8532(3)
6909.8091(3)†	10851.8139(3)
8333.6186(3)	10890.7484(3)
8333.6969(3)	10890.8210(3)
8333.7712(3)	10891.7288(6)
8334.6789(3)	11200.7458(6)
9758.8838(3)††	11200.8308(6)
9758.8107(3)††	11201.8118(3)
9787.7798(3)	

Table 3. The hump period at different epochs. Our results are consistent with a single period.

Date	period (d)
March 1991	0.0756(012)
March 1995	0.0752(150)
March 1998	0.0755(015)

3.4. "Anti-humps" and long-term hump evolution

A review of the observations of early 1998 including the discovery of "anti-humps" was given by Mennickent & Sterken (1999). Here we present a more complete analysis of the phenomenon. Fig. 9 shows in detail the events of early 1998. The light curves have been binned with a period $0\overset{\mathrm{d}}{.}0756$, accordingly to Table 3. The evolution of the hump is singular. It starts as a $0\overset{\mathrm{m}}{.}15$ absorption feature (07/01/98) then disappear from the light curve (11/01/98 and 06/02/98) and then re-appears like a small wave (07/02/98) and fully developed symmetrical hump (18/03/98 and 19/03/98). Secondary humps are also visible, with amplitude roughly 60% the main hump amplitude. On February 7 a secondary absorption hump is also visible, along with the main absorption feature. These "anti-humps" appear at the same phases where normal humps develop a month later. A close inspection to the data of February 7 reveals another alternative interpretation: the observed minima could define the base of the humps. We have rejected this hypothesis for three reasons: (1) it does not fit the ephemeris, indicating a possible shift of the hump maximum by about 0.2 cycles, (2) the peak-to-peak distance between main and secondary maxima should be 0.3 cycles instead 0.5 cycles, which is observed the other 3 nights and (3) the secondary maximum should be about 80% of the main peak, contrasting with a value of 60% observed other

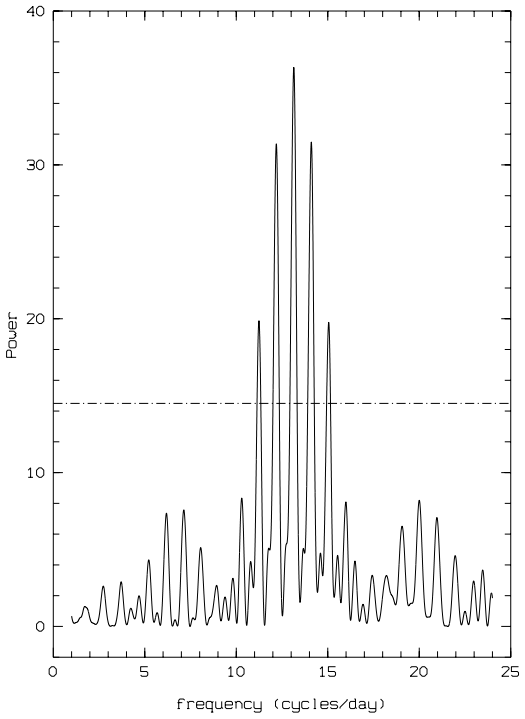

Fig. 6. The Scargle periodogram for the magnitudes of March 1991. The central peak at $0^{\rm d}.0756(12)$ is flanked by the $\pm$ 1 c d^{-1} aliases at $0^{\rm d}.071$ and $0^{\rm d}.082$. The dot-dashed line indicates the 99% confidence level.

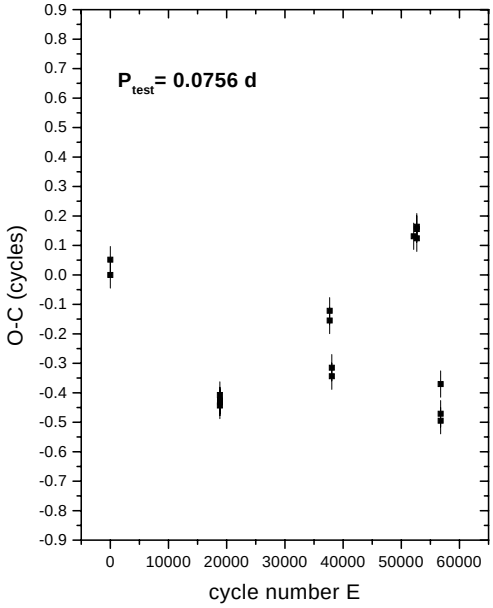

Fig. 7. O - C diagram for the times of hump maximum, with respect to a test period of $0^{\rm d}.0756$. Data are from Table 2. In principle, the figure is compatible with a non-coherent signal or with period jumps at some epochs.

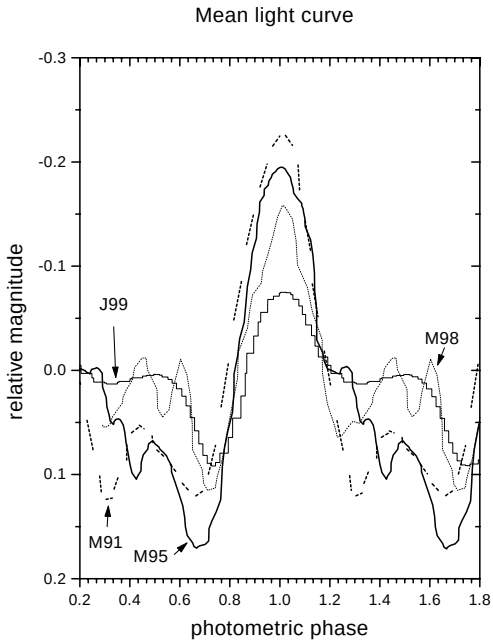

Fig. 8. Mean light curves of fully developed humps, shifted to a common phase of maximum. The curves are normalized to zero mean intensity.

nights. We provide an interpretation for this phenomenon in the next section.

Fig. 10 shows the hump's amplitude roughly anticorrelated with the nightly mean magnitude, as occurs in VW Hyi (Warner 1975). As shown in Fig. 9, this anti-correlation is not only due to the increase of hump brightness, but is also a true rise of the total systemic luminosity, through the whole orbital cycle. The outlier in Fig. 10 is a measure by Howell & Szkody (1988) which is a rather doubtful point. In fact, accordingly to these authors, since their primary goal was to obtain differential photometry – not absolute photometry – they calibrated their magnitudes using only a few standards per night. They give a formal error of $0^{\rm m}.03$ for the zero point of RZ Leo, but with so few standards observed, not in the same CCD field, it is difficult to control systematic errors due to variable seeing and atmospheric transparency. In the following, we will omit this outlier from our discussion. Returning to Fig. 10, we observe that the hump disappears when $V \approx 19$ and attains maximum amplitude when $V \approx 18.4$. Surprisingly, the hump becomes "negative" (i.e. an absorption feature) when the system drops below ≈ 19 mag. A linear least squares fit to the hump amplitude Σ yields:

$$\Sigma = 0.88(8) - 0.82(11)(V - 18) \quad (2)$$

where V refers to the nightly mean V magnitude.

4. Discussion

4.1. A moving hot spot?

Any reasonable model for the photometric variability of RZ Leo should reproduce the non-coherent humps and their amplitude variations.

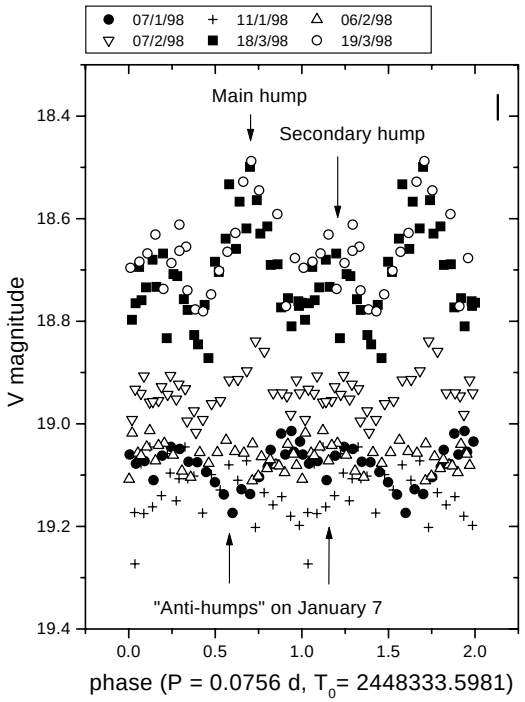

Fig. 9. Light curves of RZ Leo during early 1998 folded with a period $0^{\rm d}.0756$.

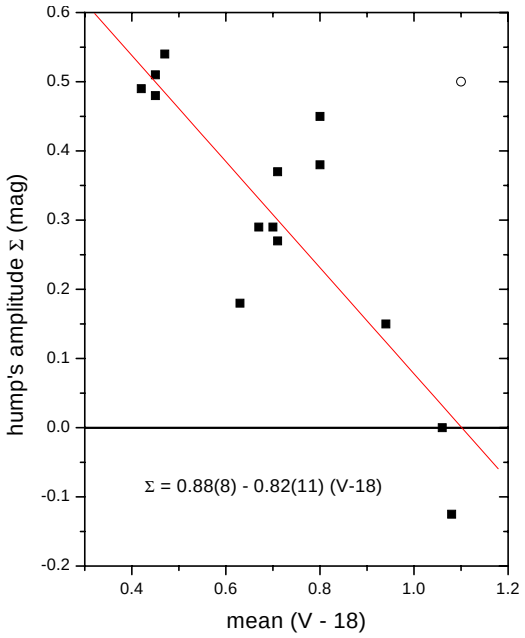

Fig. 10. Hump amplitude versus nightly mean magnitude and the best least-squares linear fit. The outlier by Howell & Szkody (1988, open circle) is discussed in the text.

It is currently assumed that the humps reflect the release of gravitational energy when the gas stream hits the accretion disk. The disk's luminosity is produced by the same process when disk gas slowly spirals towards the central white dwarf (e.g. Warner 1995a).

An explanation for the varying humps could be a hotpsot moving along the outer disk rim. A bright spot co-rotating with the binary should reflect the binary orbital period, but random translations of the hot spot along the outer disk rim should produce a non-coherent signal. Support for this view arises from the evidence of moving hot spots in some dwarf novae, e.g. KT Per (Ratering et al. 1993) and WZ Sge (Neustroev 1998).

The large scatter observed in the $O-C$ diagram of RZ Leo (up to 0.4 cycles) is atypical for dwarf novae. For example, U Gem (Eason et al. 1983), IP Peg (Wolf et al. 1993) and V 2051 Oph (Echevarría & Alvarez 1993) show quasi-cyclic period variations, of small amplitude, on time scale of years. In these cases, the $O-C$ residuals are always lower than 0.02 cycles. The interpretation of the changes observed in the above stars is still controversial.

4.2. RZ Leonis in the context of WZ Sge stars

4.2.1. Evidence for a normal α disk

In this section we analyze the events of early 1998. The observed correlation between the hump amplitude and mean brightness might provide important clues on the numerical value of the disk viscosity.

The hot spot and disk bolometric luminosity can be approximated by (Warner 1995a, Eqs. 2.21a and 2.22a):

$$L_s \approx \frac{GM_1\dot{M}_2}{r_d} \tag{3}$$

$$L_d \approx 1/2\frac{GM_1\dot{M}_d}{R_1} \tag{4}$$

where M_1 and R_1 are the mass and radius of the primary, r_d the disk's radius and $\dot{M}_2$ and $\dot{M}_d$ the mass *transfer* and mass *accretion* rates, respectively.

In the following we assume that L_s is proportional to the hump's peak luminosity and L_d is proportional to the cycle mean luminosity. The disk luminosity so defined includes some contribution from the hot spot, but it is difficult to exclude the wide and long-lasting humps from the analysis. It is apparent from Figs. 9 and 10 that the increase of hot spot luminosity is followed by an increase of the disk's luminosity. This effect seems to be true, and not simply a consequence of the hump rising.

Accordingly to Eqs. 3 and 4, the events of early 1998 may be interpreted as follows: a mass transfer burst starts at the secondary in January 1998 and then continues with increasing $\dot{M}_2$, until March 1998. The burst, evidenced in the rising of hump's luminosity in Fig. 9 triggers an increase of mass accretion rate inside the disk, as observed in the rising of the total systemic luminosity.

The time scale for matter diffusion across the accretion disk, is called the viscous time scale (Pringle 1981):

$$t_\nu \sim \frac{r_d^2}{\nu_K} \tag{5}$$

where the viscosity is given by the Shakura & Sunyaev (1973) *ansatz*:

$$\nu_K = \alpha c_s H \tag{6}$$

with H the half-thickness of the disk and c_s the sound velocity. Replacing Eq. 6 in 5 and using typical parameters H/r = 0.01, $r = 10^{10}$ cm, $c_s = 20 \times 10^5$ cm s^{-1} we obtain

$$\alpha \sim \frac{5 \times 10^5}{t_\nu} \tag{7}$$

For the diffusion process observed in RZ Leo $t_\nu \sim 6.0 \times 10^6$ s (70 days), we find α = 0.08, a common value among dwarf novae (Verbunt 1982). This value contrasts with the low α ($<<$ 0.01) invoked to explain the long recurrence times and large amplitude outbursts of some dwarf novae, in particular WZ Sge (Meyer-Hofmeister et al. 1998). Since our observations indicate a rather normal α, the long recurrence time must be explained by another cause. In this context it is worthy to mention the hypothesis of inner disk depletion.

The removal of the inner disk by the influence of a magnetosphere (Livio & Pringle 1992) or the effect of mass flow via a vertically extended hot corona above the cool disk (also referred as "coronal evaporation", Meyer & Meyer-Hofmeister 1994, Liu et al. 1997, Mineshige et al. 1998) naturally explains the long recurrence times. Spectroscopic evidence indicates that the inner disk depletion might be a common phenomenon in SU UMa stars (Mennickent & Arenas 1998, Mennickent 1999).

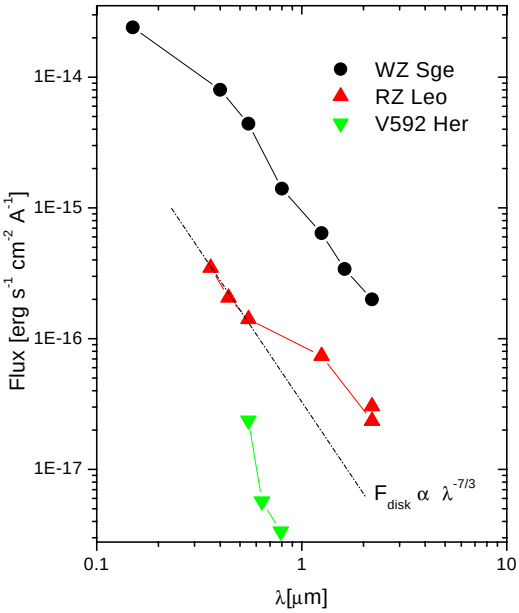

Fig. 11. The flux distribution of three large-amplitude, long cycle-length dwarf novae. Fluxes of WZ Sge are from Ciardi et al. (1998) and references therein. Those for V592 Her are based on photometry published by van Teeseling et al. (1999) and Howell et al. (1991). UBV data for RZ Leo is from this paper and JK data from Sproats et al. (1996) and Szkody (1987). The scaled flux of a steady, optically thick, accretion disk is given by the dotted line.

4.2.2. Evidence for a main sequence like secondary

It has been suggested that many large amplitude dwarf novae have bounced off from the orbital period minimum (at $\sim$ 80 min) and are evolving to longer orbital periods with very old, brown-dwarf like secondaries (Howell et al. 1997). This view is supported by the finding of undermassive secondaries in WZ Sge (Ciardi et al. 1998) and V 592 Her (van Teeseling et al. 1999) and the suspection – based on the "superhump" mass ratio – of this kind of objects in AL Com and EG Cnc (Patterson 1998). In principle, the large amplitude and long cycle length of RZ Leo suggest that this star is an ideal candidate for a post-period minimum system and therefore, for an undermassive secondary. Since superhumps have not been yet detected in this star, the only way to investigate this view is analyzing the flux distribution. We have compiled data from different sources. They are generally non-simultaneous, and may contain possibly significant variations in the emission of the CVs. However, to minimize this effect, we have excluded data taken during outburst, and we have considered data from as few sources as possible and as close together in time as possible.

The flux distributions of RZ Leo and other dwarf noave with recognized brown-dwarf like secondaries (and available photometric data) are compared in Fig. 11. The optical-IR flux of a steady disk, scaled to fit the UBV data of RZ Leo, is also shown.[2]

We find that, in contrast with that observed in the objects with undermassive secondaries, the flux distribution of RZ Leo does not drop in the red wavelengths, but rises with respect to the disk's contribution. This is expected if the secondary were a main-sequence red dwarf. In fact, the $V - K$ color of RZ Leo (viz. 3.65, Sproats el at. 1996) is representative of a main sequence M0 star (Bessell & Brett, 1988). This is consistent with the finding that most secondaries stars for cataclysmic variables with $P_o < 3$ h are close to the solar abundance main sequence defined by single field stars (Beuermann et al. 1998). The above arguments probably rule out the possibility of an undermassive secondary in RZ Leo.

Our results indicate that large amplitude – long cycle length – dwarf novae might not necessarily correspond to objects in the same evolutive stage. We have shown that, in spite of the extreme cycle length and outburst amplitude, RZ Leo cannot be properly named a *WZ Sge like star*, as suggested in the Ritter & Kolb catalogue (1998).

4.3. Anti-humps

The ratio between hot spot and disk luminosity, for the case of an optically thick, steady state accretion disk and a simple

[2] In general, the flux distribution of a CV is dominated by the accretion disk in optical wavelengths and by the secondary star in the infrared; the white dwarf and boundary layer mostly contribute to the EUV and X-ray radiation (e.g. Frank et al. 1992). The optical-IR radiation of a infinitely large, steady, optically thick disk can be approximated by a $\lambda^{-7/3}$ law (Lynden-Bell 1969).

planar bright spot on the edge of the disk, is (Warner 1995a, Eq. 2.71):

$$\frac{L_s^V}{L_d^V} = f\frac{\tan i}{1+1.5\cos i}\frac{\dot{M}_2}{\dot{M}_d}\frac{R_1}{r_d}10^{0.4(B_{sp}-B_d)} \quad (8)$$

where i is the systemic inclination, f an efficience factor ~ 1 and B_{sp} and B_d are the bolometric corrections (< 0) for the spot and disk respectively.

Roche-lobe geometry and the assumption of a disk radius 70% the Roche lobe radius (an usually good approximation for dwarf novae), yield to:

$$\frac{R_1}{r_d} \approx \frac{0.40q^{2/3}}{P_o^{3/2}(hr)} \quad (9)$$

In addition, hot spot and disk temperatures inferred for dwarf novae indicate $B_{sp} \sim B_d$ (Warner 1995a's discussion after Eq. 2.73 and references therein). Therefore we obtain:

$$\frac{L_s^V}{L_d^V} \approx h(i,q,P_o)\frac{\dot{M}_2}{\dot{M}_d} \quad (10)$$

where $h(i,q,P_o) = \frac{f\tan i}{1+1.5\cos i}\frac{0.40q^{2/3}}{P_o^{3/2}(hr)}$ is a function with a numerical value in the range 0.03–0.3 for most practical purposes. The condition of "anti-humps" is given by:

$$\frac{L_s^V}{L_d^V} < 1 \quad (11)$$

The above equations suggest that the apparition of "anti-humps" in a single system depends on the relative values of $\dot{M}_d$ and $\dot{M}_2$. In particular, for RZ Leo, assuming the orbital and photometric periods equals, a mass ratio of 0.15, i.e. representative for dwarf novae below the period gap (e.g. Mennickent et al. 1999), and a moderate inclination angle of 65^o, this occurs when $\dot{M}_2 < 6.25\dot{M}_d$ (assuming f =1). The rarity of the phenomenon indicates that $L_s < L_d$ is a condition rarely fulfilled among dwarf novae and that $\dot{M}_2$ is probably always larger or equal than $\dot{M}_d/h$. Systems with large amplitude humps are candidates for $\dot{M}_2 > \dot{M}_d/h$ whereas high inclination systems with no prominent humps (e.g. WX Cet, Mennickent 1994) are candidates for $\dot{M}_2 \sim \dot{M}_d/h$.

We can estimate the mass accretion rate from the recurrence time:

$$\dot{M}_d = \frac{880}{T_s(d)} \times 10^{15}\, g\, s^{-1} \quad T_s \leq 900\ d \quad (12)$$

(Eq. 37 by Warner 1995b). Using a supercycle length $T_s > 2$ yr we obtain $\dot{M}_d < 1.2\times10^{15}$ g s^{-1}. This implies that $\dot{M}_2 < 7.5\times 10^{15}$ g s^{-1} is required to develop "anti-humps". This condition is easily satisfied if the mass transfer rate is driven by gravitational radiation, as expected for a dwarf novae below the period gap. In this case, using the system parameters given above, we estimate:

$$\dot{M}_2^{GR} = 2.2 \times 10^{15}\, g s^{-1} \quad (13)$$

from Eq. 9.20 by Warner (1995a).

Since the mass accretion rate $\dot{M}_d$ is proportional to the viscosity (e.g. Cannizzo et al. 1998), an extremely low α disk is not a good site for developing "anti-humps". The reason is that, in this case, the condition imposed on the mass transfer rate to satisfy Eq. 11 is too strong, requiring, probably, unrealistic low $\dot{M}_2$ values. Therefore the presence of "anti-humps" in RZ Leo is consistent with the normal α found in the previous section.

5. Conclusions

- The light curve of RZ Leo during a time interval of 11-years is characterized by highly variable humps.
- A non-coherent photometric period of $0^{\rm d}.0756(2)$ is consistent with the data.
- The hump amplitude is anti-correlated with the stellar mean brightness.
- A new phenomenon was reported: the presence of "anti-humps" when the system is faint.
- Anti-humps might result from a regime of very low mass transfer rate and normal alpha disks.
- Non-coherent humps are compatible with a non-steady hot spot.
- The rapid response of the accretion disk to the enhanced mass transfer rate evidenced by the phenomena of early 1998 (Fig. 9) suggests a disk with a normal viscosity parameter $\alpha \sim 0.08$.
- The possibility of an undermassive secondary is rejected by arguments concerning the observed optical and infrared flux distribution.

Acknowledgements. This work was partly supported by Fondecyt 1971064 and DI UdeC 97.11.20-1. Support for this work was also provided by the National Science Foundation through grant number GF-1002-98 from the Association of Universities for Research in Astronomy, Inc., under NSF Cooperative Agreement No. AST-8947990. C. Sterken acknowledges a research grant of the Fund for Scientific Research Flanders (FWO).

References

Armitage P.J., Livio M., 1998, MNRAS 297, L81
Bessell M.S., Brett J.M., 1988, PASP 100, 1134
Beuermann K., Baraffe I., Kolb U., at al., 1998, A&A 339, 518
Bisikalo D.V., Boyarchuk A.A., Kuznetsov O.A., et al., 1998, Astronomy Reports 42, 33
Cannizzo J.K., Shafter A.W., Wheeler J.C., 1988, ApJ 333, 227
Ciardi D.R., Howell S.B., Hauschildt P.H., et al., 1998, ApJ 504, 450
Cristiani S., Duerbeck H., Seitter W.C., 1985, IAU Circ 4027
Eason E.L.E., Africano J.L., Klimke A., et al., 1983, PASP 95, 58
Echevarria J., Alvarez M., 1993, A&A 275, 187
Frank J., King A., Raine D., 1992, Accretion Power in Astrophysics. 2nd edition, Cambridge University Press
Hessman F.V., 1999, ApJ 510, 867
Howell S. B., Dobrzycka D., Szkody P., et al., 1991, PASP 103, 300
Howell S.B., 1992, In: Howell S.B. (ed.) Astronomical CCD Observing and Reduction Techniques. ASP Conference Series Vol. 23, p. 105
Howell S.B., Szkody P., 1988, PASP 100, 224
Howell S.B., Mitchell K.J., Warnock III A., 1988, AJ 95, 247
Howell S.B., Rappaport S., Politano M., 1997, MNRAS 287, 929

Liu B.F., Meyer F., Meyer-Hofmeister E., 1997, A&A 328, 247
Livio M., Pringle J.E., 1992, MNRAS 259, 23L
Lynden-Bell D., 1969, Nat 223, 690
Mennickent R.E., 1994, A&A 285, 979
Mennickent R.E., 1999 A&A 348, 364
Mennickent R.E., Arenas J., 1998, PASJ 50, 333
Mennickent R.E., Sterken C., 1999, IBVS 4672, 1
Mennicker R.E., Matsumoto K., Arenas J., 1999, A&A 348, 466
Meyer-Hofmeister E., Meyer F., Liu B.F., 1998, A&A 339, 507
Meyer F., Meyer-Hofmeister E., 1994, A&A 288, 175
Mineshige S., Liu B., Meyer F., et al., 1998, PASJ 50, L5
Misselt K.A., 1996, PASP 108, 146
Neustroev V.V., 1998, Astronomy Reports 42, 748
Patterson J., 1998, PASP 110, 1132
Pringle J.E., 1981, ARA&A 19, 137
Ratering C., Bruch A., Diaz M., 1993, A&A 268, 694
Ritter H., Kolb U., 1998, A&AS 129, 83
Shakura N.I, Sunyaev R.A., 1973, A&A 24, 337
Scargle J.D., 1982, ApJ 263, 835
Sproats L.N., Howell S.B., Mason K.O., 1996, MNRAS 282, 1211
Szkody P., 1992, In: Vogt N. (ed.) The Viña del Mar Workshop on Cataclysmic Variable Stars. ASP Conference Series Vol. 29, p. 42
Szkody P., Howell S.B., 1991, ApJS 78, 537
Szkody P., 1987, ApJS 63, 685
Verbunt F., 1982, Space Sci. Rev. 32, 379
van Teeseling A., Hessman F.V., Romani R.W., 1999, A&A 342, L45
Vanmuster T., Howell S.B., 1996, In: Evans A., Wood J.H. (eds.) Cataclysmic Variables and Related Objects. Astrophysics and Space Science Library Vol. 208, Kluwer Academic Publishers, p. 63
Vogt N., Bateson F.M., 1982, A&AS 48, 383
Warner B., 1975, MNRAS 170, 219
Warner B., 1995a, Cataclysmic Variable Stars. Cambridge University Press
Warner B., 1995b, Ap&SS 226, 187
Wolf S., Mantel K.H., Horne K., et al., 1993, A&A 273, 160
Wolf S., Barwig H., Bobinger A., et al., 1998, A&A 332, 984